Winter 2021

Macro-and Micromechanical Modelling Of HA-Elastin Scaffold Fabricated Using Freeze Drying Technique

Matin Mohammadzadeh Rad
Amirkabir University of Technology

Saeed Saber-Samandari
Amirkabir University of Technology

Mojtaba Sadighi
Amirkabir University of Technology

Lobat Tayebi
Marquette University, lobat.tayebi@marquette.edu

Mohammad Mohammadi Aghdam
Amirkabir University of Technology

See next page for additional authors

RESEARCH ARTICLE

Macro-and micromechanical modelling of HA-Elastin scaffold fabricated using freeze drying technique

Matin Mohammadzadeh Rad[1], Saeed Saber-Samandari[2], Mojtaba Sadighi[1], Lobat Tayebi[3], Mohammad Mohammadi Aghdam[1], Amirsalar Khandan[2,*]

[1] Department of Mechanical Engineering, Amirkabir University of Technology, Tehran, Iran

[2] New Technologies Research Center, Amirkabir University of Technology, Tehran, Iran

[3] School of Dentistry, Marquette University, Milwaukee, USA

ARTICLE INFO

Article History:
Received 2020-05-16
Accepted 2020-08-11
Published 2021-02-01

Keywords:
Nanocomposite
Scaffold
Mechanical property
Wollastonite-HA ceramic
Micromechanical model

ABSTRACT

Since osteomyelitis is a serious and dangerous disease, it requires immediate treatment with antibiotics or bone substitute replacement in orthopedic surgeries. Therefore, a porous polymeric-ceramic was fabricated using hydroxyapatite (HA) and polymethylmethacrylate (PMMA) composed with elastin as an ideal scaffold for bone tissue engineering applications. The current study is aimed at investigating the effects of various amounts of elastin biopolymer on porous bio-nanocomposite scaffold using the freeze-drying (FD) technique. The morphology and phase analysis of the prepared scaffold are analyzed using scanning electron microscope (SEM) and X-ray diffraction (XRD) techniques. The biological performance of the porous tissue is evaluated in simulated body fluid (SBF) and sodium chloride (SC) solution. The tensile test is used to measure the elastic modulus and tensile strength of the porous tissue before soaking in the SBF. The obtained result is simulated using micromechanical model from the experimental values. The elastic modulus of samples decreases from 1.18 MPa to 0.69 MPa, and porosity evaluation is in the range of 70-85% with addition of 10 wt% and 15 wt% elastin to PMMA-HA bio-nanocomposite. The biological behavior indicates that a thick apatite layer precipitate on the surface of the sample with 10 wt% elastin beside increases alkaline group with constant pH concentration. According to the obtained porosity and elastic modulus results, suitable micromechanical model is assessed. The comparison of micromechanical model is assessed, and error rate was less than 10%; therefore, optimum model is introduced as the best micromechanical model for porous bone substitute.

How to cite this article
*Mohammadzadeh Rad M., Saber-Samandari S., Sadighi M., Tayebi L., Mohammadi Aghdam M., Khandan A.S.. Macro-and micromechanical modelling of HA-Elastin scaffold fabricated using freeze drying technique. J. Nanoanalysis., 2021; 8(1): -15. DOI: 10.22034/jna.***.*

INTRODUCTION

In order to transfer the drug-containing nanoparticles in the porous scaffold structure and damaged bone area, it is necessary to construct a suitable scaffold with appropriate pore size [1-3]. The designed porous scaffold is not only considered as a carrier and substrate for the nanoparticles, but—with appropriate physicochemical properties—can also repair the affected bone area[3-6]. In this regard, natural polymers will be used to create homogeneous structures with nanoparticles. Because of an increasing trend in degenerative diseases of hard tissues, there is a need to use new methods to fabricate new bone composition and speed up the bone healing. Therefore, new material composition can facilitate this process. Hydroxyapatite (HA), as a bioactive ceramic, is widely used in medicine and dentistry with suitable fracture toughness and compression strength value [7-10]. The HA with the chemical formula ($Ca_5(PO_4)_3(OH)$) is one of the most known

* Corresponding Author Email: *amir_salar_khandan@yahoo.com*

calcium phosphates (CaPs) in its families [11-13]. The structural tissue of HA is very similar to that of bone's HA ($Ca_{10}(PO_4)_5(OH)$). The phosphate, calcium materials and HA are especially ideal for bone implanting due to the similarity between their chemical formulae with the bone tissue and their biocompatibility, which do not create inflammation and having the capacity to produce bone cells [14]. However, due to its weak mechanical properties (being tender and fragile), such materials cannot be used as implants or organs with heavy load bearing. Polymethylmethacrylate (PMMA) is one of the best degenerative biopolymers, which has a proper resistance against the unwanted chemical reactions. PMMA is able to overcome the chemical and physical property shortcomings and weaknesses of HA as the constructive organ close to the main microstructure of the human bone. In addition, PMMA biopolymer can show great biocompatibility with the bone in the biological environment, as orthopedic surgeons commonly use PMMA as bone cement. The preparation of this commercial bone cement can be used to enhance the mechanical performance of the bone mechanism along with the elastin that is made of collagen strands and elastic strands (Elastin). The elastin is similar to collagen strands in collagen protein [13, 14]. These strands are scattered largely in the connective tissues of the body that are supported by an underlying substance, called glycosaminoglycans (Glycosaminoglycans). Elastin is a key extracellular matrix (ECM) protein, which makes the tissues and organs flexible and enhances its tensile property. Elastin is more than 100-fold more flexible than collagens, therefore, the main function of elastin is to increase the tissues' tensile strength [15-17]. The composition of this substance with the PMMA can lead to the curing of cement in an orthopedic surgery, in which the MMA monomer in the liquid form and PMMA polymer in the powder form is poured on the polymer while using monomer; the polymerization is completed very quickly. One of the most important advantages of this bone cement is that as a load is applied, the cement can absorb the energy and either diminish the load or impede the transfer to the surgery position. PMMAs are used because they are non-toxic, along with having low costs, easy processing, biocompatibility and minimal inflammation in bone tissues. Additionally, they have high resistance to therapeutic applications, including nasal surgery, dental fillers and orthopedic applications. In cartilage, collagen is encapsulated in a gel-like underlying material, and a multi-composite of various properties can be obtained [13, 14]. Regarding the importance of this subject, numerous studies have been conducted in this field. Tavakol et al. [15], Offeddu et al. [16] and Liu et al. [17] investigated the mechanical and biological performance properties of the bone scaffold. The non-absorbable thermoset composites with toxic effects cannot be used in human bone, while the thermoplastic polymers have a suitable biological response, such as formation with the application of heat during the surgery [18-26]. In the current study, we fabricate a novel PMMA-HA bio-nanocomposite reinforced with elastin polymer for orthopedics approaches using the freeze-drying technique. Then, the mechanical and biological properties of the samples are investigated. The obtained results are then used to predict the micromechanical model of the samples.

MATERIALS AND METHODS

Materials preparation

Hydroxyapatite with a chemical formula of $Ca_5(PO_4)_3(OH)$, purity of 97% and particle size less than 100 nm from CAM bioceramic was used. In this study, PMMA with the density of 1.200 g/cm^3 is obtained from the Merck Co. Germany. The PMMA bone cement was used for clinical applications and strength in the artificial joint in hip and knee arthroplasty to stabilize the prosthesis. The bone cement is basically made of polymethylmethacrylate powder and monomethylmethacrylate (MMA) liquid, which was purchased from Merck company with high purity. In addition, it shows great biocompatibility with the bone which makes it as a potential candidate for this work. In the current study, the elastin with 96% purity was produced by Pasteur Company. The prepared elastin has a thickness of about 100 nm, with 5 nm thickness with high molecular weight with approved biocompatibility [23-25]. The purchased elastin shows proper mechanical properties. The calcium silicate nanopowder (wollastonite: WS) ($CaSiO_3$) showed better mechanical and biological properties compared to HA powder for application directly on transplants within the living bones. It belongs to the calcium silicate group and received lots of attention due to its high biocompatibility and mechanical features. The high bioactivity of WS is due to having a silicone ion in its microstructure, which plays a large role in new formations with

Table 1. Mechanical and biological properties of porous bio-nanocomposite scaffolds.

Sample	Elastic Modulus (MPa)	Apatite Formation (%)
0 wt%	1.08±0.05	0.20
5 wt%	0.63±0.03	0.26
10 wt%	1.18±0.05	0.29
15 wt%	0.69±0.03	0.31

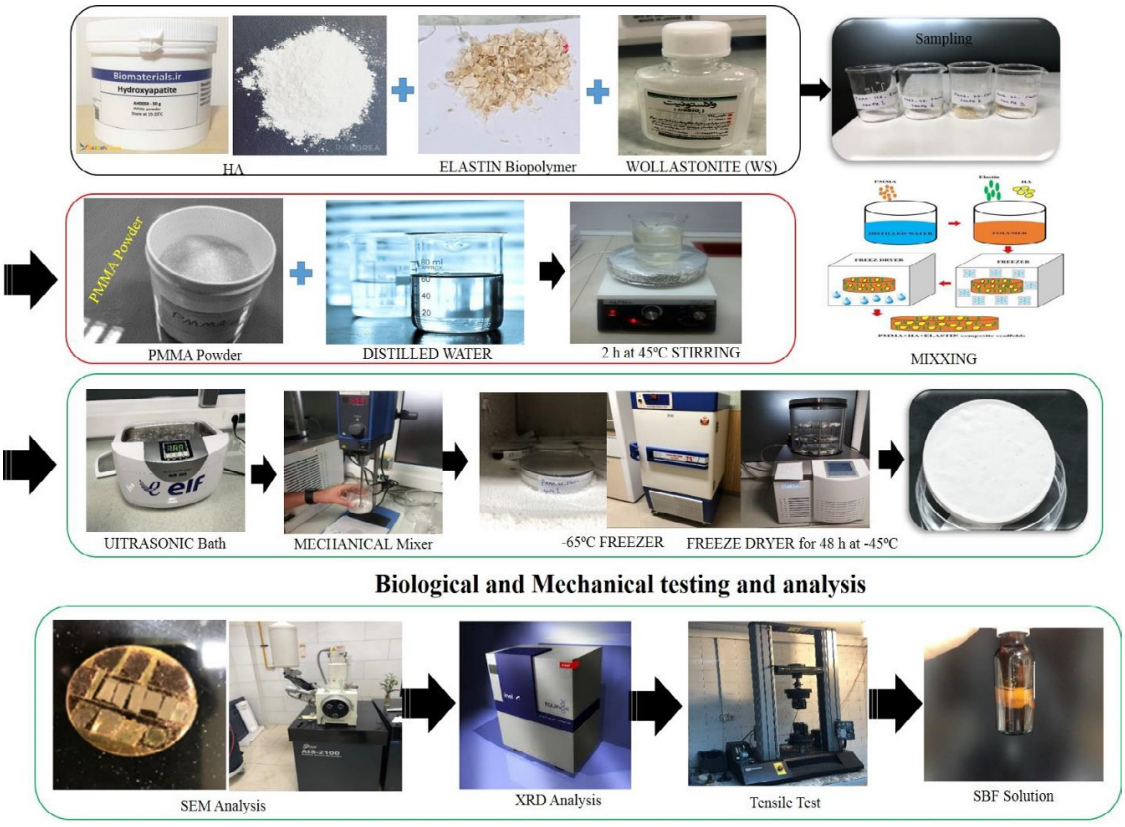

Fig.1. Schematic of fabrication of novel PMMA-HA containing various amounts of elastin for bio-nanocomposite scaffolds.

the metabolic process. The WS was synthesized using mechanical activation (MA) method and combination of $CaCO_3$ and SiO_2 with standard stochiometric values. The synthetic Wollastonite was biocompatible with 99% purity and size of 80-100 nm. Calcium silicate bioceramic has been used as a bone replacement in the biomedical applications [24].

Preparation of bio-nanocomposite scaffolds

For dissolution of the polymeric bases in the elastic additive, 10 CC of double distilled water was used, and the added materials were fully dissolved by putting the compound on magnetic stirrer for 60 min. As shown in Table 1 and Fig. 1, the schematic and process of bio-nanocomposite in which the materials are mixed with different elastic weight percentages. The prepared solution is fabricated using 0.1 g wollastonite (WS, mechanical activation process for synthesize), 0.1 g MMA, 2.5 g PMMA, 2.5 g HA (98% purity, CAM Netherlands, 50-100 nm) and elastin with weight percentages of 0, 5, 10, and 15 wt% were added to the bio-nanocomposites solution. There are several common methods for fabrication of porous scaffold with porous microstructures, such as fiber bonding, solvent casting, gas foaming, 3D printing, space holder and phase separation techniques. However, in this study, the freeze-drying (FD) technique has been used for fabrication of the porous bone scaffold

made of PMMA matrix and HA reinforcement [26]. In order to prevent deposition, the porous bio-nanocomposite scaffold with the elastin with 0 wt%, 5 wt%, 10 wt% and 15 wt% weight percentages were added to the PMMA-HA composition on the magnetic stirrer for 60 min at 50°C. Then the homogenized solution was kept in the -65°C freezer machine (Made by Zhale Industrial Group) for 24 hours. Then, the freeze sample were removed from the freezer and inserted into the freeze-drying machine (DORSATECH Company, Tehran, Iran) at -45°C at 0.1 bar at CRLAB. For the fabrication of the porous bio-nanocomposite scaffold, the freeze-drying machine was set at 0.8 kW and a voltage of 220 VAC, which was equipped with vacuum solenoid valve to extend vacuum pump life. The samples were put inside the freeze drier machine in order to obtain a consistent and porous sample. On the other hand, it reduces the stresses caused by shrinkage during drying process and also prevents the particle settling, adhesion and mass buildup in the main drying process.

Materials characterization

XRD Analysis

The x-ray diffraction (XRD) analysis was conducted to monitor the structure and phase identification (XRD, Philips X pert- MPD System) for the synthesized powder and the composite scaffold with Equinox 300 machine in the 2θ range of 10 to 80 degrees under 40 kV and 30 mA).

SEM Analysis

The SEM analysis is one of the mostly used types of equipment for surface analysis. It evaluates the microstructure of the materials through surface scanning by electron beam, and acts similar to the optical microscopes, but with much higher resolution and much larger depth of field. Perhaps the most important characteristic of the scanning electron microscope is the 3D demonstration of its images, due to having larger field depth. For identification, morphological evaluation and formation of the deposits of composite scaffold, along with the analysis of existing materials, the SEM method—using a device made by SERON Technologies Inc in Korea, Tehran Polytechnic—was used with gold coating sputter on the samples surface.

Tensile strength test

The tensile test is used to measure tensile strength of the porous bio-nanocomposite scaffold containing various amounts of elastin in the PMMA-HA. In the current study, the INSTRON5566 device was used under uniaxial loading. The obtained results from the test are usually used to choose a substance for controlling the quality and predicting how a substance reacts under other types of forces. Also, the following properties can be determined by such measurements: elastic modulus, Poisson's ratio, yield stress and strain hardening.

Apatite formation evaluation

The biological response and biocompatibility of the samples were investigated using simulated body fluid (SBF), according to the Kokubo solution, and physiological saline for 28 days in the benmary bath. The bioactivity behavior of the sample was predicted using analytical models and SEM image and EDX analysis in the SBF solution. The samples were soaked in 10 ml SBF in the plastic falcon with a smooth surface. Also, the biocompatibility of the samples—as one of the most important criteria for scaffold in bone engineering—were incorporated into the porous scaffold [25-28]. The biocompatibility of scaffold should not have an immunological response or swelling in the body. On the other hand, the porous bio-nanocomposite scaffold must be bio-degenerative so that it can enable the cell to produce extracellular matrix [3, 4]. The biodegradation rate of samples evaluated in the physiological saline (0.9% sodium chloride) as sterile and nonpyrogenic as a solution for intravenous administration. The osmolarity is 308 m.mol/L (calc.) and the pH is 5.6 with no bacteriostat, antimicrobial agent or added buffer. The biodegradation rate of the porous scaffold may provide hypotonic or isotonic concentrations of sodium chloride, which is suitable for parenteral maintenance [29].

Micromechanical model simulation

Recently, the use of porous scaffold for damaged bone repair has been increased in the orthopedic field. Since obtaining the mechanical properties of porous scaffold in the laboratory-based methods are time-consuming and expensive, numerous researchers have put their efforts into the mathematical methods to predict the correlation between the elastic modulus and porosity value. Different micromechanical methods have been suggested for describing porosity effect on the elastic modulus of bone scaffold. In the current

Table 2. Mechanical and physical properties used in micromechanical models [30].

Spherical	Oval	Shape of pores
0.798	0.818	m
2.25	1.65	n
0.166	0.221	a
0.604	0.84	b

study, besides investigation of the porosity using image-J and SEM images, the porosity values were used in the micromechanical model to evaluate the effect of porosity vs. elastic modulus. The obtained equations can be used for quick estimation of elastic modulus and Poisson's ratio according to previous micromechanical models [30, 31]. It should be noted that in the following equations, E, υ, k, μ, ϕ and $\rho\rho$ are elastic modulus, Poisson's ratio, bulk modulus, shear modulus, porosity percentage and density, respectively. Also, the subtitles 's' and 'p' are indicative of the related quantity to the order of the substrate (the non-porous material from the same substance) and the porous material [31, 32]. The Dewey model (DM) has provided a linear equation (1) for calculation of elastic modulus of the porous scaffolds.

$$\frac{E_p}{E_s} = 1 - \xi\phi \tag{1}$$

In which the ξ coefficient is obtained from equation (2).

$$\xi = \frac{(1-\nu_s)(27+15\nu_s)}{(2(7-5\nu_s))} \tag{2}$$

The Gibson model (GM) has proposed equation (3) for evaluation of elastic modulus of porous bio-nanocomposite scaffold fabricated using the freeze drying technique.

$$\frac{E_p}{E_s} = \frac{\rho_p}{\rho_s} = (1-\phi)^{\eta} \tag{3}$$

In which η value is 2 and 3 for open and close porous architecture, respectively.

Roberts and Garboczi Model (RGM) have proposed equations (4) and (5) for the calculation of elastic modulus and Poisson's ratio of porous materials.

$$\frac{E_p}{E_s} = (1-\frac{\phi}{m})^n \tag{4}$$

$$\nu_p = a + (1-\frac{\phi}{b})(\nu_s - a) \tag{5}$$

Parameters *m*, *n*, *a* and *b* are experimental results with different modes that provided in Table 2.

Wang and Tseng model (WTM) proposed a model for the estimation of the effective mechanical properties of dual-phase composite materials containing spherical particles with random distribution. According to this model, the effective bulk modulus and shear modulus of porous material have been expressed through equations (6) and (7) [31, 32].

$$\kappa_p = \kappa_s\left\{1+\frac{30(1-\nu_s)\phi(3\Lambda+2\Theta)}{3\alpha+2\beta-10(1+\nu_s)\phi(3\Lambda+2\Theta)}\right\} \tag{6}$$

$$\mu_p = \mu_s\left\{1+\frac{30(1-\nu_s)\phi\Theta}{\beta-4(4-5\nu_s)\phi\Theta}\right\} \tag{7}$$

In which the equations (8) to (11) are as follows:

$$\alpha = 2(5\nu_s - 1) \tag{8}$$

$$\beta = -7 + 5\nu_s \tag{9}$$

$$\Lambda = \frac{(-12+18\nu_s-15\nu_s^2)\phi}{4(-7+5\nu_s)^2} \tag{10}$$

$$\Theta = \frac{1}{2} + \frac{(107-98\nu_s+65\nu_s^2)\phi}{16(-7+5\nu_s)^2} \tag{11}$$

Elastic modulus and Poisson's ratio of the porous material can be obtained by inserting (6) and (7) into equations (12) and (13).

$$E_p = \frac{9\kappa_p\mu_p}{3\kappa_p+\mu_p} \tag{12}$$

$$\nu_p = \frac{3\kappa_p-2\mu_p}{2(3\kappa_p+\mu_p)} \tag{13}$$

The dilute estimation method (DEM) has been originally proposed for porous bio-nanocomposite scaffolds with a very tiny bulk percentage of nanoparticles. Therefore, the dilute estimation method can be used for obtaining the mechanical properties of the porous materials with low porosity percentage (ϕ<<1). Assuming that the pores had a spherical shape, the bulk and shear moduli of a porous material can be obtained by equations (14) and (15) using DEM model [30].

$$\kappa_p = \kappa_s (1-\phi(1+\frac{3\kappa_s}{4\mu_s})) \tag{14}$$

$$\mu_p = \mu_s (1-5\phi\frac{3\kappa_s+4\mu_s}{9\kappa_s+8\mu_s}) \tag{15}$$

By obtaining the bulk and shear modulus and inserting them in equations (12) and (13), elastic modulus and Poisson's ratio of the porous material can be obtained. The differential scheme (DS) aims to overcome the $\phi \ll 1$ limitation, which is the reason for the limited application of DEM. The DEM was used in each phase to obtain the effective mechanical properties of the porous material. First, a very small percentage of porosity was applied on the ingredient, and the properties of the obtained material were calculated by equations (14) and (15). The materials' distribution and porosity value would lead to obtaining two coupled equations, (16) and (17), for the calculation of bulk and shear modulus of the porous material [30].

$$\frac{(1+\frac{4\mu_s}{3\kappa_s})(\frac{\mu_p}{\mu_s})^3}{2-(1-\frac{4\mu_s}{3\kappa_s})(\frac{\mu_p}{\mu_s})^{\frac{3}{5}}} = (1-\phi)^6 \tag{16}$$

$$\frac{\mu_p}{\mu_s} = \frac{(1-\frac{4\mu_p}{3\kappa_p})^{\frac{5}{3}}}{(1-\frac{4\mu_s}{3\kappa_s})^{\frac{5}{3}}} \tag{17}$$

It should be noted that equations (16) and (17) are true when $\nu_s > 0.2$. For calculation of bulk and shear modulus when $\nu_s > 0.2$, the coupled differential equations (18) and (19) have been used [30]:

$$\frac{(1+\frac{4\mu_s}{3\kappa_s})(\frac{\mu_p}{\mu_s})^3}{2+(\frac{4\mu_s}{3\kappa_s}-1)(\frac{\mu_p}{\mu_s})^{\frac{3}{5}}} = (1-\phi)^6 \tag{18}$$

$$\frac{\mu_p}{\mu_s} = \frac{(\frac{4\mu_p}{3\kappa_p}-1)^{\frac{5}{3}}}{(\frac{4\mu_s}{3\kappa_s}-1)^{\frac{5}{3}}} \tag{19}$$

RESULTS AND DISCUSSION

XRD analysis

The XRD pattern is beneficial in determining the structure and crystallization of the polymer matrices. XRD analysis is performed, then the diffraction patterns of pure HA, pure PMMA, pure elastin and show the spectrometer of XRD from porous bio-nano composites with 0 wt%, 5 wt%, 10 wt%, and 15 wt% of elastin in PMMA-HA in Fig. 2(a-g). The XRD pattern (Fig. 2(a)), single-phase observations of HA can be seen, while no extra stable phases can be seen. Also, an appropriate consistency between diffraction peaks could be seen with JCPDS: -432 (this standard is related to X pert software to XRD device). The main peaks of HA powder's XRD determined the formation of HA powder due to its similarity with bone apatite's for medical approaches. Fig. 2(b) shows two broad peaks at angles 2θ=9.16° and 19.12°, which are ascribed to PMMA. Fig. 2(c) shows diffraction peaks at 2θ=10.49° and 15.33° and sharp shoulder at 2θ=20.11°, which are attributed to elastin. Fig. 2(d) shows that the 0 wt% sample of elastin had a series of peaks at 11, 15 and 20°, which are indicative of the ceramic polymer behavior of the material. These peaks confirm the presence of crystal networks of PMMA and HA throughout the bio-nano composite. Two peaks can be seen at about 12 and 22° in the 5 wt% and 10 wt% samples of elastin in Fig. 2(e, f). These peaks are related to the crystal zone of elastin nanoparticles. Fig. 2(g) shows the 15 wt% sample of elastin has two peaks at about 25 and 33°. With an increase in elastin percentage, the polymer percentage of the material drastically increases, and a change in crystal structure of the material occurs. In other words, the material becomes amorphous, since elastin is a natural polymer that can create significant phase changes.

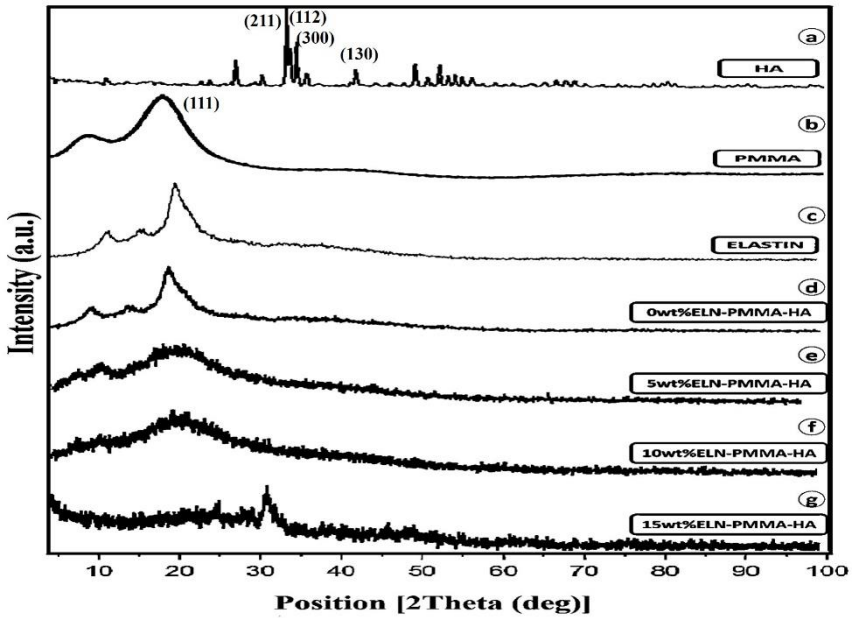

Fig. 2. XRD pattern of (a) pure HA, (b) PMMA, (c) elastin and composite scaffold containing (d) 0 wt% ELN, (e) 5 wt% ELN, (f) 10 wt% ELN, (g) 15 wt% ELN in PMMA-HA.

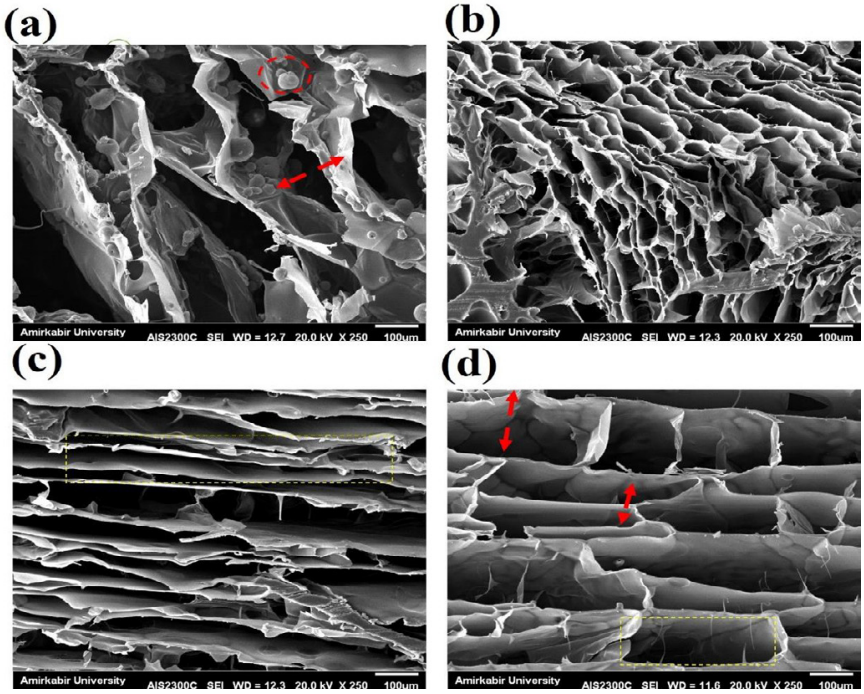

Fig. 3. SEM images of porous bio-nanocomposite scaffolds with (a) 0 wt%, (b) 5 wt%, (c) 10 wt% and (d) 15 wt% ELN in PMMA-HA.

SEM analysis

Fig. 3 (a-d) shows the SEM image of porous scaffold with B-shaped, square and multifaceted pores, and that the samples have a porous structure, most of which have a porosity of about 70-85% of open type in around 100-150 μm. The structure of the pores is honeycomb and interconnected, which could lead to an increase in the stability and mechanical strength.

These pores and cavities are interconnected,

and thus, they provide the cells with nutrients and oxygen for growth, as seen in Fig. 3(a). The sample with 0 wt% elastin present more spherical HA particles pasted to the polymer wall of PMMA, however in 3(b, c) and 3(d), with the increase in elastin, the HA particles also settle in 10 wt% sample. Additionally, the spherical microstructure of the shape is evident, which leads to the increase of tensile strength, since the tensile concentration was reduced. Regarding Fig. 4(a-d), the nanoparticles were analyzed by Image-J software.

Regarding the Fig. 5, the more the elastin weight percentage increased, the lower the number of pores and cavities; the size of the pores is also decreased. Fathi et al. [33] showed that the addition of filling and reinforcing powder to the polymer scaffold leads to a decrease in porosity and size of the pores.

Tensile strength result

The mechanical strength of the porous bio-nanocomposite scaffold is one of the most important characteristics of efficiency and load bearing of this bone substitute replacement [34-38]. The mechanical strength is the most important factor in maintaining and stability of the scaffold after placing it in an *in vivo* environment, because these new tissues are subject to different loads from various directions in the host bone. As the load increases after a short time, the bone scaffold may encounter microcracks and, consequently, fractures toughness of the host tissue. This tensile strength of the porous tissue depends on different factors—such as the elastic modulus, porosity percentage, the geometry of the materials, the size of the nanoparticles and fracture toughness—as well as

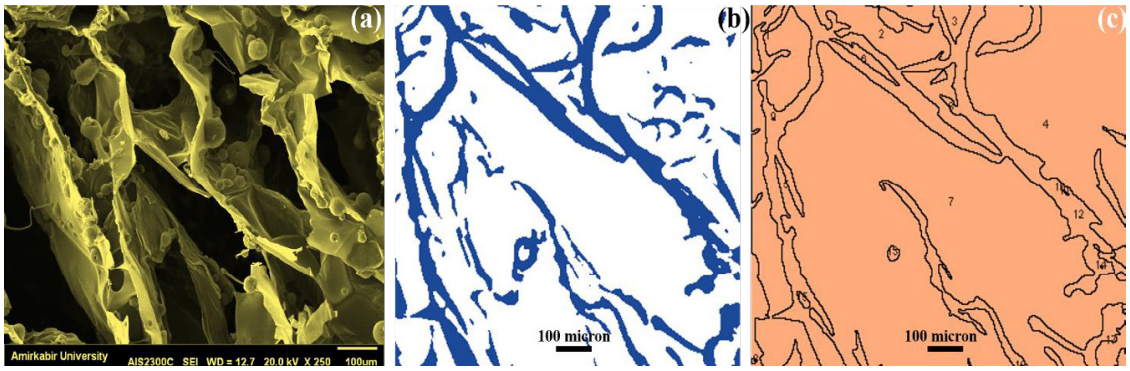

Fig. 4. (a) SEM image of porous bio-nanocomposite scaffold, (b) PMMA-HA layer-by-layer tissue containing HA particle and (c) surface of scaffold without layers.

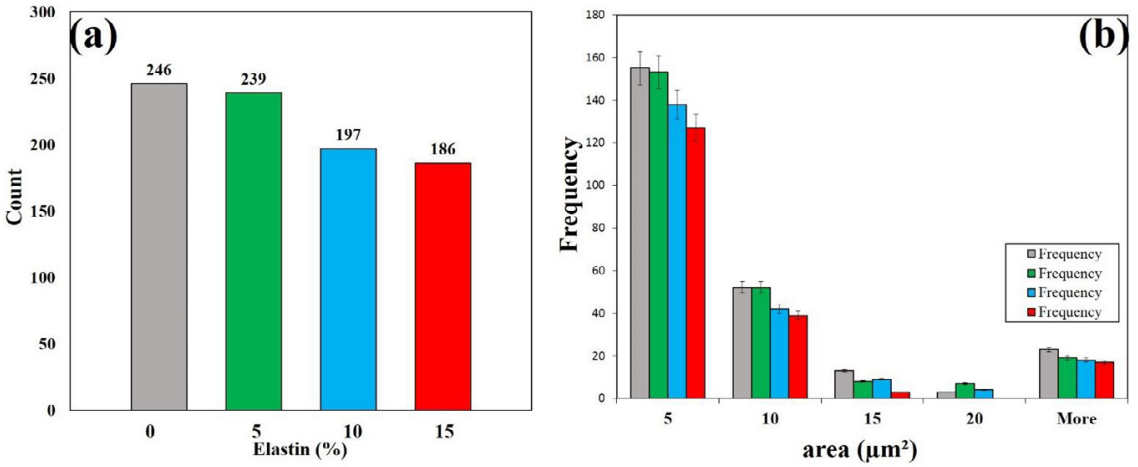

Fig. 5. Comparison of the area distribution of porous bio-nanocomposite containing various amounts of elastin in PMMA-HA in the weight loss test and using Image-J software.

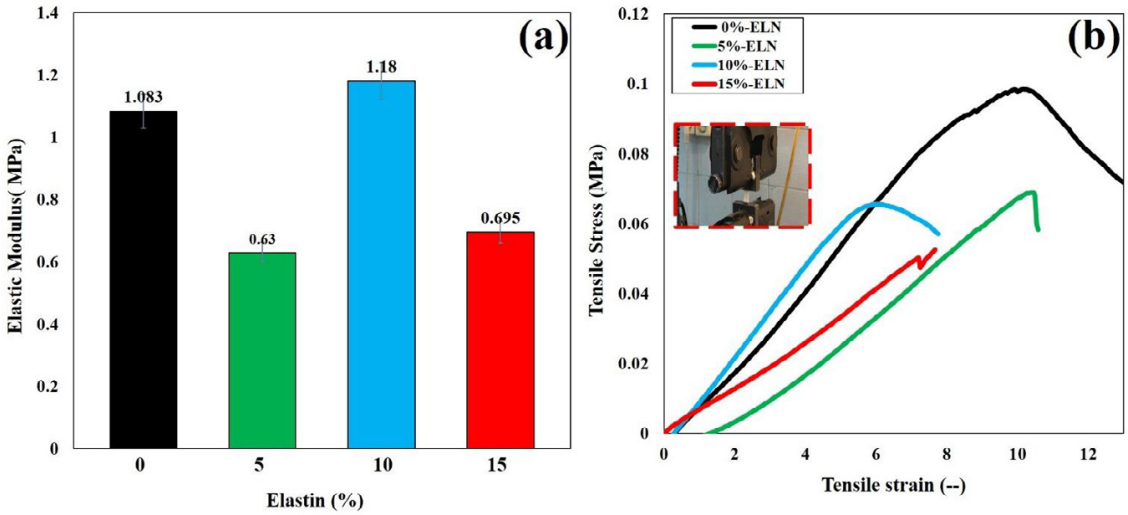

Fig. 6. Comparison of the elastic modulus and stress-strain diagram of porous bio-nanocomposite scaffolds containing various amounts of elastin in PMMA-HA composite.

the ratio of these elements. The tensile strength test can partially determine the initial strength of the scaffolds. However, the scaffold in the *in vivo* situation showed more strength over time due to the creation of deposits on its surface and chemical mineralization on its surface [39-42] .

The stress-strain curves of the porous scaffold represent three main portions—the elastic zone, the plastic or wax-like zone, in which the change in strain are not linearly proportionate to the stress, and the density zone, which occurs after the initial drop in stress point [43-51]. The elastic modulus (the slope of the initial linear part of the graph) and tensile strength (maximum stress) of the samples are represented in Fig. 6. Generally, it can be determined that the mechanical properties of the porous scaffold depend on the elastin crystallization feature. As seen, with addition of 5 wt% elastin, the mechanical properties of the porous bio-nanocomposite decrease from 1.083±0.05 MPa to 0.63±0.03 MPa. However, the addition of 10 wt% elastin can improve the tensile strength of the architecture from 0.63±0.03 MPa to 1.18±0.05 MPa. Also, further investigations show sample 5 wt% and 15 wt% have similar trends, in which the tensile strength decreases from 1.18±0.05 MPa to 0.695±0.03 MPa. The mechanical performance can be attributed to the scaffold porosity, which is itself another factor effective mechanical properties (i.e. low porosity has led to the increase in mechanical properties of the scaffold). Regarding Fig. 6, it is seen that increasing 10 wt% elastin can increase the the strength of the sample, while with the reinforcement above this percentage, their strength decreases. Diba et al. [31] showed that the addition of reinforcement to the polymer scaffold has led to the increase in strength due to reduction in porosity, pores size, and the reinforcing and filling powder. However, the increase in reinforcement above 10 wt% leads to powder agglomeration, and the uniformity of the powder distribution decreases. Therefore, with higher increase in elastin percentage, the strength is decreased[51-53].

Apatite formation, weight loss and pH change analysis

Apatite layer prevents the release of Ca^{2+} ions from the porous scaffold in the SBF. The use of hydroxyapatite—due to its special structure and low crystallinity—may increase the strength of the porous scaffold after soaking in the SBF solution. A hypertonic concentration of physiological saline can be used to treat severe salt depletion syndrome. In water, sodium chloride dissociates into sodium (Na^+) and chloride (Cl^-) ions. The principal cation of the extracellular fluid is sodium (Na^+), which contributes largely to the therapy of electrolyte disturbances. Chloride (Cl^-), on the other hand, has an essential role in buffering action in red blood cells during oxygen and carbon dioxide exchange. Mainly, the kidney controls the distribution and excretion of sodium (Na^+) and chloride (Cl^-) in

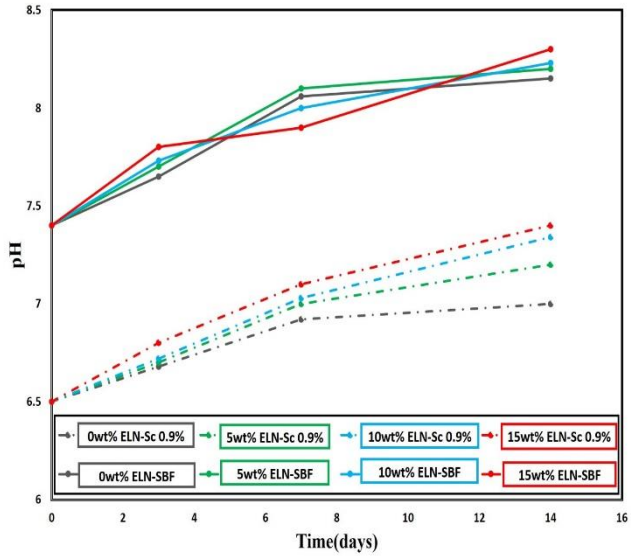

Fig. 7. pH changes of porous bio-nanocomposite scaffolds with various amount of elastin in PMMA-HA soaked in the SBF and physiological solution.

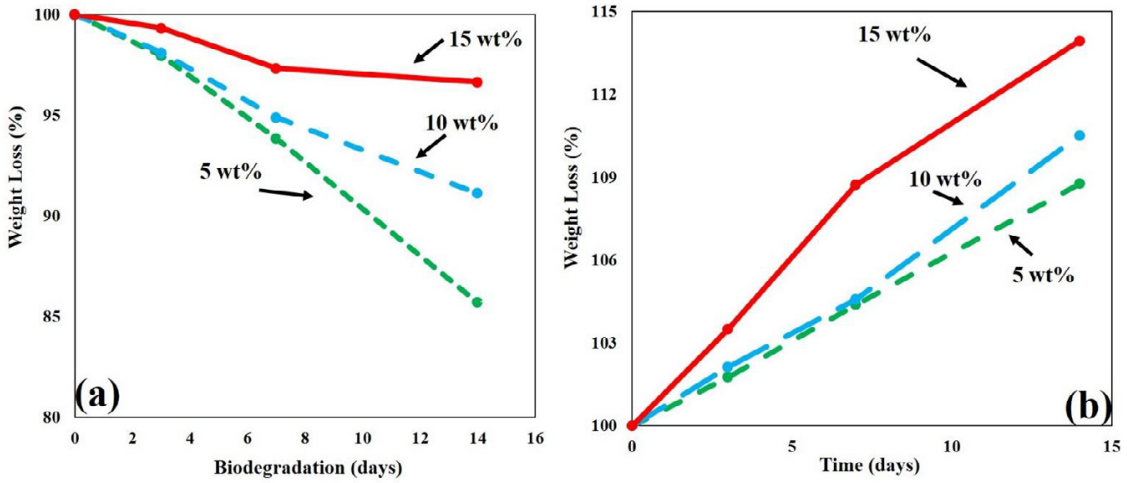

Fig. 8. Weight loss changes of porous bio-nanocomposite scaffolds with various amount of elastin in PMMA-HA in (a) SBF solution and (b) physiological saline.

order to maintain a balance between intake and output. Fig. 7 shows the pH changes in the SBF and physiological saline of the sample containing the porous bio-composite scaffold with various amounts of 0 wt%, 5 wt%, 10 wt% and 15 wt% elastin. The results of pH changes indicate that as the sample soaks in the SBF and physiological saline, more alkaline and apatite layer forms on the porous scaffold surface. The ICP-AES analysis of the sample demonstrates that pH changes from 7.3 to 8.1 with high calcium and silica saturation in the SBF, which is related to the HA ($Ca_{10}(PO_4)_6(OH)_2$ and wollostonite ($CaSiO_3$) in the matrix of the composite. The apatite formation of the sample's changes from 0.25 to 0.31, demonstrating about 15% more apatite formation on the surface of the sample with higher amount of elastin. However, the biodegradation rate of the sample decreases from 0.18 to 0.12 with an increase of elastin to the bio-nanocomposite.

As shown in Fig. 8(a), the weight changes in bio-nanocomposite scaffolds for sample with 5

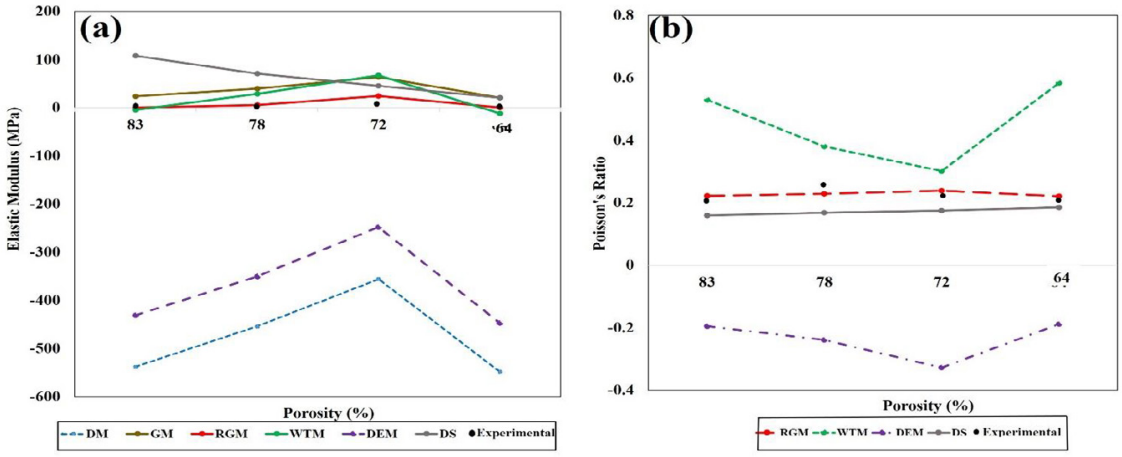

Fig. 9. (a) Elastic modulus of experimental and analytical results with various porosities and (b) Poisson's ratio of different porosities.

wt% elastin lost its microstructure topology in the consecutive days and in the 7th day. Also, the results show that a high dissolution rate of 14.29% is reported. Also, the samples with 0 wt%, 10 wt% and 15 wt% elastin have a slow dissolubility rate as after 14 days, within less than 4% solubility percentage. As seen, all the scaffolds have lost their weight in the SBF solution after 28 days. The reason behind this phenomenon is likely the increase in penetration weight and settlement of the NaCl in PMMA and HA microstructure[53-57]. Hence, there is a low reaction of salt in the dextrose saline with the samples and high reactivity in the SBF saline. Finally, the sample with 10 wt% of biopolymer shows better chemical, mechanical and biological response.

Micromechanical model

Fig. 9 shows the elastic modulus of the prepared novel porous scaffolds with different porosities. The obtained results of micromechanical model show the DM and DEM model are not appropriate for the samples with high porosity percentage. Also, the following models have been proposed for the estimation of elastic modulus in dilute state (for low porosities). The DS model is applicable for the samples with lower amount of porosity. It should be noted that the DS model has been recommended for the obviation of the limitations of DEM in predicting the mechanical properties of high porous scaffolds. Thus, according to the micromechanical logics for the porous bio-nanocomposite with higher porosity than 50%, the DS can appropriately predict the elastic modulus of samples [27, 58-61].

Fig. 9(a) shows the maximum error of the obtained values with DS method—near 40%—for porous bio-nanocomposites for all the samples. The micromechanical performance of GM, RAM and WTM models in prediction of the elastic modulus are almost similar. Fig. 9(b) illustrates the obtained values for Poisson's ratio vs. various porosity percentages for porous bio-nanocomposites used in the RGM, WTM, DEM and DS models. It should be noted that other methods mentioned in the study are not able to calculate the Poisson's ratio alteration with various porosity value. The micromechanical result in the DEM method shows that it has weak behavior in prediction of porosity value and elastic modulus with representing negative Poisson's ratio. Other micromechanical models, like Wang and Tseng method, cannot predict Poisson's ratio for the sample with more than 80% porosity, which cannot be suitable for prediction of elastic modulus and Poisson ratio. Among the all the models that have been applied, the best performance in the calculation of Poisson's ratio for 64% porosity belongs to Roberts and Gerboczi method (with a maximum error of 6.2%). On the other hand, most of the proposed models are based on Finite Element Method (FEM), and they have been less addressed theoretically. Fig. 10 illustrates the comparison of Poisson ratio vs. density for samples containing various amount of elastin in PMMA-HA fabricated using the freeze drying technique. Fig. 10 shows that the Poisson ratio of the porous scaffold increases as the elastin is added to the PMMA-HA.

Fig. 11 represents the bone apatite formation

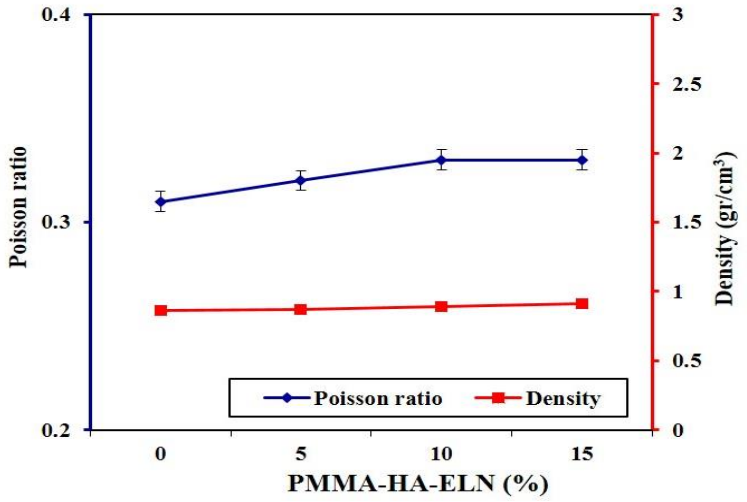

Fig. 10. Comparison of Poisson ratio vs. density for samples containing various amount of elastin in PMMA-HA fabricated using freeze drying technique.

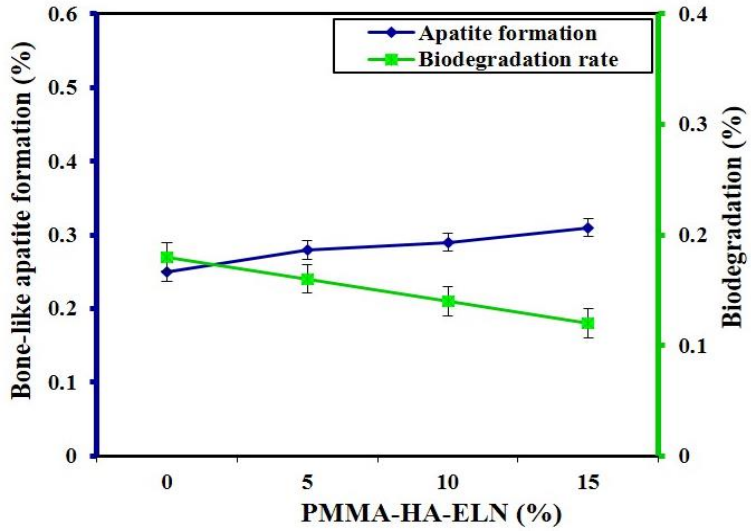

Fig. 11. Bone apatite formation vs. degradation rate of nanocomposite containing various amount of elastin soaking in SBF solution for 28 days.

vs. degradation rate of porous bio-nanocomposite containing various amount of elastin soaking in the SBF solution for 28 days. The apatite formation increases while the degradation rate decreases. Fig. 11 shows that the sample initially degrades in the first and second week, however, degradation rate decreases in the third and final weeks. The soaking analysis shows that with addition of elastin, the apatite formation depends on degradation rate reversely.

The reason for these changes is specific mechanical performance and lattice constant of the nanoparticles. The density of the composite remains constant with increasing elastin polymer to the PMMA-HA composite.

CONCLUSION

The main objective of this work was to fabricate a novel PMMA-HA-ELASTIN porous scaffold for tissue engineering application. The novel PMMA-HA-ELASTIN was fabricated using freeze drying technique for bone substitute application.

The mechanical and biological properties of the porous scaffold were measured for use in the micromechanical model for evaluation and prediction of the effect of porosity on elastic modulus of porous bio-nanocomposite. The SEM image shows that the specimen with 10 wt% elastin increased the tensile strength and fracture toughness of the porous bio-nanocomposite. The SEM images also show that the samples have a porous microstructure with open porous channel and that the microstructure of the porous architecture is honeycomb and interconnected. These cavities in the porous scaffold are interconnected, which help the nutrients and oxygen to be transferred into the cells. Addition of 5 wt% elastin may decrease the porosity percentage of the porous architecture. The evaluation of phase characterization using XRD shows that the crystallinity and crystal size increase in the samples. The elastic modulus, fracture toughness and tensile strength of the porous scaffolds depends on amount of elastin to the PMMA-HA bio-nanocomposite. The mechanical performance of the sample containing 10 wt% elastin decreases from 1.083 MPa to 0.63 MPa, however, the sample with 10 wt% elastin shows better tensile strength, increasing from 0.63 MPa to 1.18 MPa. The tensile strength value of the porous scaffold decreases 15% with addition of 15 wt% elastin. The biological response of the porous scaffold is enhanced with addition of elastin biopolymer in the SBF and physiological saline, which represent a better alkaline group and constant pH changes. The mechanical behavior of porous scaffolds is simulated using micromechanical models. The obtained results of porous bio-nanocomposite scaffolds indicate suitable performance in GM, RGM and WTM models and have the potential application in prediction of elastic modulus of the specimen.

CONFLICT OF INTEREST STATEMENT

All authors declare that no conflicts of interest exist for the publication of this manuscript.

REFERENCES

[1] Joneidi Yekta, H., Shahali, M., Khorshidi, S., Rezaei, S., Montazeran, A.H., Samandari, S.S., et al. Mathematically and experimentally defined porous bone scaffold produced for bone substitute application. Nanomedicine Journal. 2018, 5, 227-34.

[2] Saber-Samandari, S., Yekta, H., Saber-Samandari, S. Effect of iron substitution in hydroxyapatite matrix on swelling properties of composite bead. JOM. 2015, 9, 19-25.

[3] Najafinezhad, A., Abdellahi, M., Saber-Samandari, S., Ghayour, H., Khandan, A. Hydroxyapatite-M-type strontium hexaferrite: a new composite for hyperthermia applications. Journal of Alloys and Compounds. 2018, 734, 290-300.

[4] Saber-Samandari, S., Saber-Samandari, S. Biocompatible nanocomposite scaffolds based on copolymer-grafted chitosan for bone tissue engineering with drug delivery capability. Materials Science and Engineering: C. 2017, 75, 721-32.

[5] Eslami, H., Tahriri, M., Moztarzadeh, F., Bader, R., Tayebi, L., Eslami, H., et al. Nanostructured hydroxyapatite for biomedical applications: from powder to bioceramic. Journal of the Korean Ceramic Society. 2018, 55, 597-607.

[6] Saber-Samandari, S., Yekta, H., Ahmadi, S., Alamara, K. The role of titanium dioxide on the morphology, microstructure, and bioactivity of grafted cellulose/hydroxyapatite nanocomposites for a potential application in bone repair. International journal of biological macromolecules. 2018, 106, 481-8.

[7] Raisi, A., Asefnejad, A., Shahali, M., Doozandeh, Z., Kamyab Moghadas, B., Saber-Samandari, S., & Khandan, A. (2020). A soft tissue fabricated using freeze-drying technique with carboxymethyl chitosan and nanoparticles for promoting effects on wound healing. Journal of Nanoanalysis.

[8] Kordjamshidi, A., Saber-Samandari, S., Nejad, M.G., Khandan, A. Preparation of novel porous calcium silicate scaffold loaded by celecoxib drug using freeze drying technique: Fabrication, characterization and simulation. Ceramics International. 2019, 45, 14126-35.

[9] Aghdam, H.A., Sheikhbahaei, E., Hajihashemi, H., Kazemi, D., Andalib, A. The impacts of internal versus external fixation for tibial fractures with simultaneous acute compartment syndrome. European Journal of Orthopaedic Surgery & Traumatology. 2019, 29, 183-7.

[10] Safari, M.B., Tabrizi, A., Hassani, E., Aghdam, H.A., Shariyate, M.J. Painful scoliosis secondary to posterior rib osteoid osteoma: a case report and review of literature. Journal of Orthopedic and Spine Trauma. 2017, 3.

[11] Motififard, M., Vakili, M., Moezi, M. Short-Time Influence of Totah Hip Arthroplasty on Patients with Sever Hip Ostheoarthritis. Journal of Isfahan Medical School. 2013, 31.

[12] Moeini, M., Barbaz Isfahani, R., Saber-Samandari, S., Aghdam, M.M. Molecular dynamics simulations of the effect of temperature and strain rate on mechanical properties of graphene–epoxy nanocomposites. Molecular Simulation. 2020, 46, 476-86.

[13] Maghsoudlou, M.A., Isfahani, R.B., Saber-Samandari, S., Sadighi, M. Effect of interphase, curvature and agglomeration of SWCNTs on mechanical properties of polymer-based nanocomposites: Experimental and numerical investigations. Composites Part B: Engineering. 2019, 175, 107119.

[14] Ayatollahi, M.R., Moghimi Monfared, R., Barbaz Isfahani, R. Experimental investigation on tribological properties of carbon fabric composites: effects of carbon nanotubes and nano-silica. Proceedings of the Institution of Mechanical Engineers, Part L: Journal of Materials: Design and Applications. 2019, 233, 874-84.

[15] Tavakol, S., Nikpour, M.R., Amani, A., Soltani, M., Rabiee, S.M., Rezayat, S.M., et al. Bone regeneration based on nano-hydroxyapatite and hydroxyapatite/chitosan nanocomposites: an in vitro and in vivo comparative study.

Journal of nanoparticle research. 2013, 15, 1373.
[16] Offeddu, G.S., Ashworth, J.C., Cameron, R.E., Oyen, M.L. Multi-scale mechanical response of freeze-dried collagen scaffolds for tissue engineering applications. journal of the mechanical behavior of biomedical materials. 2015, 42, 19-25.
[17] Liu, X., Rahaman, M.N., Hilmas, G.E., Bal, B.S. Mechanical properties of bioactive glass (13-93) scaffolds fabricated by robotic deposition for structural bone repair. Acta biomaterialia. 2013, 9, 7025-34.
[18] Hashemi, S.A., Esmaeili, S., Ghadirinejad, M., Saber-Samandari, S., Sheikhbahaei, E., Kordjamshidi, A., et al. Micro-Finite Element Model to Investigate the Mechanical Stimuli in Scaffolds Fabricated via Space Holder Technique for Cancellous Bone. ADMT Journal. 2020, 13, 51-8.
[19] Ghadirinejad, M., Atasoylu, E., Izbirak, G., Gha-Semi, M. A Stochastic Model for the Ethanol Pharmacokinetics. Iranian journal of public health. 2016, 45, 1170.
[20] Salmani, M. M., Hashemian, M., Yekta, H. J., Nejad, M. G., Saber-Samandari, S., & Khandan, A. (2020). Synergic Effects of Magnetic Nanoparticles on Hyperthermia-Based Therapy and Controlled Drug Delivery for Bone Substitute Application. JOURNAL OF SUPERCONDUCTIVITY AND NOVEL MAGNETISM.
[21] Farazin, A., Aghadavoudi, F., Motififard, M., Saber-Samandari, S., Khandan, A. Nanostructure, molecular dynamics simulation and mechanical performance of PCL membranes reinforced with antibacterial nanoparticles. Journal of Applied and Computational Mechanics. 2020.
[22] Mirzaalian, M., Aghadavoudi, F., Moradi-Dastjerdi, R. Bending Behavior of Sandwich Plates with Aggregated CNT-Reinforced Face Sheets. Journal of Solid Mechanics. 2019, 11, 26-38.
[23] Sahmani, S., Saber-Samandari, S., Shahali, M., Yekta, H.J., Aghadavoudi, F., Montazeran, A.H., et al. Mechanical and biological performance of axially loaded novel bio-nanocomposite sandwich plate-type implant coated by biological polymer thin film. Journal of the mechanical behavior of biomedical materials. 2018, 88, 238-50.
[24] Moradi-Dastjerdi, R., Aghadavoudi, F. Static analysis of functionally graded nanocomposite sandwich plates reinforced by defected CNT. Composite Structures. 2018, 200, 839-48.
[25] Khandan, A., Ozada, N., Saber-Samandari, S., Nejad, M.G. On the mechanical and biological properties of bredigite-magnetite (Ca7MgSi4O16-Fe3O4) nanocomposite scaffolds. Ceramics International. 2018, 44, 3141-8.
[26] Ghayour, H., Abdellahi, M., Nejad, M.G., Khandan, A., Saber-Samandari, S. Study of the effect of the Zn 2+ content on the anisotropy and specific absorption rate of the cobalt ferrite: the application of Co 1− x Zn x Fe 2 O 4 ferrite for magnetic hyperthermia. Journal of the Australian Ceramic Society. 2018, 54, 223-30.
[27] Bagherifard, A., Joneidi Yekta, H., Akbari Aghdam, H., Motififard, M., Sanatizadeh, E., Ghadiri Nejad, M., ... & Khandan, A. (2020). Improvement in osseointegration of tricalcium phosphate-zircon for orthopedic applications: an in vitro and in vivo evaluation. Medical & Biological Engineering & Computing, 1-13.
[28] Esmaeili, S., Shahali, M., Kordjamshidi, A., Torkpoor, Z., Namdari, F., Samandari, S.S., et al. An artificial blood vessel fabricated by 3D printing for pharmaceutical application. Nanomedicine Journal. 2019, 6, 183-94.
[29] Beladi, F., Saber-Samandari, S., Saber-Samandari, S. Cellular compatibility of nanocomposite scaffolds based on hydroxyapatite entrapped in cellulose network for bone repair. Materials Science and Engineering: C. 2017, 75, 385-92.
[30] Aghdam, H.A., Sanatizadeh, E., Motififard, M., Aghadavoudi, F., Saber-Samandari, S., Esmaeili, S., et al. Effect of calcium silicate nanoparticle on surface feature of calcium phosphates hybrid bio-nanocomposite using for bone substitute application. Powder Technology. 2020, 361, 917-29.
[31] Diba, M., Kharaziha, M., Fathi, M.H., Gholipourmalekabadi, M., Samadikuchaksaraei, A. Preparation and characterization of polycaprolactone/forsterite nanocomposite porous scaffolds designed for bone tissue regeneration. Composites Science and Technology. 2012, 72, 716-23.
[32] Farazin, A., Aghdam, H.A., Motififard, M., Aghadavoudi, F., Kordjamshidi, A., Saber-Samandari, S., et al. A polycaprolactone bio-nanocomposite bone substitute fabricated for femoral fracture approaches: Molecular dynamic and micro-mechanical Investigation. J Nanoanaly. 2019.
[33] Fathi, M.H., Hanifi, A., Mortazavi, V. Preparation and bioactivity evaluation of bone-like hydroxyapatite nanopowder. Journal of materials processing technology. 2008, 202, 536-42.
[34] Zhang, K., Van Le, Q. Bioactive Glass Coated Zirconia for Dental Implants: a review. Journal of Composites and Compounds. 2020, 2, 10-7.
[35] Acciaioli, A., Falco, L., Baleani, M. Measurement of apparent mechanical properties of trabecular bone tissue: Accuracy and limitation of digital image correlation technique. Journal of the Mechanical Behavior of Biomedical Materials. 2020, 103, 103542.
[36] Monshi, M., Esmaeili, S., Kolooshani, A., Moghadas, B.K., Saber-Samandari, S., Khandan, A. A novel three-dimensional printing of electroconductive scaffolds for bone cancer therapy application. Nanomedicine Journal. 2020, 7, 138-48.
[37] Tamjidi, S., Esmaeili, H., Moghadas, B.K. Application of magnetic adsorbents for removal of heavy metals from wastewater: a review study. Materials Research Express. 2019, 6, 102004.
[38] Kamyab Moghadas, B., Azadi, M. Fabrication of Nanocomposite Foam by Supercritical CO2 Technique for Application in Tissue Engineering. Journal of Tissues and Materials. 2019, 2, 23-32.
[39] Shahriari, S., Houshmand, B., Razavian, H., Khazaei, S., Abbas, F.M. Effect of the combination of enamel matrix derivatives and deproteinized bovine bone materials on bone formation in rabbits' calvarial defects. Dental research journal. 2012, 9, 422.
[40] Hasheminia, D., Razavi, S.M., Nazari, H., Khazaei, S., Soleimanzadeh, P. Systemic supplement with resveratrol increased bone formation in ratsâ alveolar socket Aumento de la formaciÃ³n Ã³sea en el hueso alveolar de rata con suplemento sistÃ© mico con resveratrol. International Journal of Morphology. 2018, 36, 391-4.
[41] Ghasemi, E., Abedian, A., Iranmanesh, P., Khazaei, S. Effect of type of luting agents on stress distribution in the bone surrounding implants supporting a three-unit fixed dental prosthesis: 3D finite element analysis. Dental research

journal. 2015, 12, 57.
[42] Khazaei, M., Bozorgi, A., Khazaei, S., Khademi, A. Stem cells in dentistry, sources, and applications. Dental Hypotheses. 2016, 7, 42.
[43] Khandan, A., Karamian, E., Bonakdarchian, M. Mechanochemical synthesis evaluation of nanocrystalline bone-derived bioceramic powder using for bone tissue engineering. Dental Hypotheses. 2014, 5, 155.
[44] Zhang, X., Zhou, X., Hu, D. Combining 3-dimensional degradable electrostatic spinning scaffold and dental follicle cells to build peri-implant periodontium. Dental Hypotheses. 2013, 4, 118.
[45] Esmaeili, S., Aghdam, H.A., Motififard, M., Saber-Samandari, S., Montazeran, A.H., Bigonah, M., et al. A porous polymeric–hydroxyapatite scaffold used for femur fractures treatment: fabrication, analysis, and simulation. European Journal of Orthopaedic Surgery & Traumatology. 2020, 30, 123-31.
[46] Razavi, M., Khandan, A. Safety, regulatory issues, long-term biotoxicity, and the processing environment. In: Nanobiomaterials Science, Development and Evaluation, Elsevier, 2017, pp. 261-79.
[47] Sahmani, S., Khandan, A., Esmaeili, S., Saber-Samandari, S., Nejad, M.G., Aghdam, M.M. Calcium phosphate-PLA scaffolds fabricated by fused deposition modeling technique for bone tissue applications: Fabrication, characterization and simulation. Ceramics International. 2020, 46, 2447-56.
[48] Sahmani, S., Shahali, M., Nejad, M.G., Khandan, A., Aghdam, M.M., Saber-Samandari, S. Effect of copper oxide nanoparticles on electrical conductivity and cell viability of calcium phosphate scaffolds with improved mechanical strength for bone tissue engineering. The European Physical Journal Plus. 2019, 134, 7.
[49] Karamian, E., Nasehi, A., Saber-Samandari, S., Khandan, A. Fabrication of hydroxyapatite-baghdadite nanocomposite scaffolds coated by PCL/Bioglass with polyurethane polymeric sponge technique. Nanomedicine Journal. 2017, 4, 177-83.
[50] Sarraf, M., Dabbagh, A., Razak, B.A., Nasiri-Tabrizi, B., Hosseini, H.R.M., Saber-Samandari, S., et al. Silver oxide nanoparticles-decorated tantala nanotubes for enhanced antibacterial activity and osseointegration of Ti6Al4V. Materials & Design. 2018, 154, 28-40.
[51] Baradaran, S., Nasiri-Tabrizi, B., Shirazi, F.S., Saber-Samandari, S., Shahtalebi, S., Basirun, W.J. Wet chemistry approach to the preparation of tantalum-doped hydroxyapatite: Dopant content effects. Ceramics International. 2018, 44, 2768-81.
[52] Sahmani, S., Khandan, A., Saber-Samandari, S., Aghdam, M.M. Effect of magnetite nanoparticles on the biological and mechanical properties of hydroxyapatite porous scaffolds coated with ibuprofen drug. Materials Science and Engineering: C. 2020, 110835.
[53] Abd-Khorsand, S., Saber-Samandari, S., Saber-Samandari, S. Development of nanocomposite scaffolds based on TiO2 doped in grafted chitosan/hydroxyapatite by freeze drying method and evaluation of biocompatibility. International journal of biological macromolecules. 2017, 101, 51-8.
[54] Saber-Samandari, S., Gross, K.A. Amorphous calcium phosphate offers improved crack resistance: A design feature from nature? Acta biomaterialia. 2011, 7, 4235-41.
[55] Saber-Samandari, S., Gross, K.A. Effect of angled indentation on mechanical properties. Journal of the European Ceramic Society. 2009, 29, 2461-7.
[56] Sahmani, S., Khandan, A., Saber-Samandari, S., Aghdam, M.M. Vibrations of beam-type implants made of 3D printed bredigite-magnetite bio-nanocomposite scaffolds under axial compression: Application, communication and simulation. Ceramics International. 2018, 44, 11282-91.
[57] Sahmani, S., Khandan, A., Saber-Samandari, S., Aghdam, M.M. Nonlinear bending and instability analysis of bioceramics composed with magnetite nanoparticles: Fabrication, characterization, and simulation. Ceramics International. 2018, 44, 9540-9.
[58] Enab, T.A., Fouda, N., Eldesouky, I. Numerical study of functionally graded hip implants with different second-generation titanium alloys. Journal of Applied and Computational Mechanics. 2020.
[59] Taharou, B., Merdji, A., Hillstrom, R., Benaissa, A., Roy, S., Della, N., et al. Biomechanical Evaluation of Bone Quality Effect on Stresses at Bone-Implant Interface: A Finite Element Study. Journal of Applied and Computational Mechanics. 2020.
[60] Raisi, A., Asefnejad, A., Shahali, M., Doozandeh, Z., Kamyab Moghadas, B., Saber-Samandari, S., Khandan, A. (2020). A soft tissue fabricated using freeze-drying technique with carboxymethyl chitosan and nanoparticles for promoting effects on wound healing. Journal of Nanoanalysis, (), -. doi: 10.22034/jna.2020.1895736.1196.
[61] Ayatollahi, M. R., Barbaz Isfahani, R., & Moghimi Monfared, R. (2017). Effects of multi-walled carbon nanotube and nanosilica on tensile properties of woven carbon fabric-reinforced epoxy composites fabricated using VARIM. Journal of Composite Materials, 51(30), 4177-4188.